Biochimica et Biophysica Acta, 942 (1988) 215–219
Elsevier

BBA 74057

The catalytic mechanism of gastric H^+/K^+-ATPase: simulations of pre-steady-state and steady-state kinetic results

Peter Brzezinski [a], Bo G. Malmström [a], Pia Lorentzon [b] and Björn Wallmark [b]

[a] *Department of Biochemistry and Biophysics, Chalmers University of Technology and University of Göteborg, Göteborg and* [b] *Department of Biology, Hässle Gastrointestinal Research Laboratories, Mölndal (Sweden)*

(Received 25 February 1988)

Key words: ATPase, H^+/K^+-; Steady-state kinetics; Phosphoenzyme intermediate; Gastric mucosa; (Hog)

A reaction cycle for the gastric H^+/K^+-ATPase is proposed. This has been used to simulate the results from four types of pre-steady-state and steady-state kinetic experiments: (1) the K^+ dependence of the dephosphorylation of the phosphoenzyme; (2) the rate of phosphorylation of the enzyme by ATP at different concentrations; (3) the effect of ATP concentration on the steady-state rate of ATP hydrolysis; (4) the phosphoenzyme levels in the steady state at various ATP concentrations. A single set of equilibrium and rate constants can be used to reproduce the results from all four sets of experiments quite well. It is suggested that the steady-state rate equation is nonhyperbolic because ATP can react with the enzyme in both the E_1 and the E_2 state, but with a lower affinity in E_2. No single step is by itself limiting the maximum turnover rate.

Introduction

The gastric H^+/K^+-ATPase [1], which is responsible for the acid secretion from the parietal cells in the mucosa, belongs to the class of E_1E_2 transport ATPases, which also includes, for example, the Na^+/K^+-ATPase [2] and the sarcoplasmic Ca^{2+}-ATPase [3]. ATP processing in this group of enzymes occurs via an acyl phosphate intermediate, in which the phosphate is covalently linked to an aspartyl residue of the protein. Furthermore, this intermediate exists in two distinct states, designated $E_1 \sim P$ and E_2-P, respectively.

Catalytic cycles for the H^+/K^+-ATPase have been proposed [4–6], based on the extensive kinetic information available. Essential steps in these mechanistic schemes are an H^+-dependent kinase reaction, leading to formation of $E_1 \sim P$, and a K^+-dependent phosphatase reaction, in which E_2-P is hydrolyzed, as well as interconversions from $E_1 \sim P$ to E_2-P and from E_2 back to E_1.

In this communication we show that a catalytic cycle of this type can be used to simulate a variety of kinetic results. These include the dependence of the rate of the phosphatase reaction on the concentration of K^+, the concentration of the phosphate intermediate in the steady state and its pre-steady-state rate of formation as a function of the ATP concentration, and the nonhyperbolic dependence of the steady-state rate on the ATP concentration.

Materials and Methods

The gastric H^+/K^+-ATPase was prepared from hog stomachs according to previously published

Abbreviation: Pipes, 1,4-piperazinediethanesulfonic acid.

Correspondence: B.G. Malmström, Department of Biochemistry and Biophysics, Chalmers University of Technology, S-412 96 Göteborg, Sweden.

methods [7]. In short, the enzyme was prepared from homogenized mucosa by differential and zonal density gradient centrifugation, followed by free-flow electrophoresis. The H^+/K^+-ATPase-containing vesicles were lyophilized and stored at $-80\,^\circ C$ prior to use.

[γ-^{32}P]ATP was purchased from Amersham/Searle, and ATP was obtained from Sigma. All other reagents were of the highest purity available.

The phosphoenzyme levels in the steady state were determined as described by Wallmark et al. [4]. All other experimental results were adapted from Ref. 4.

Simulations of the pre-steady-state results were made on an IBM 3081 computer, which solved the kinetic equations by stepwise integration with an extended Runge-Kutta method. The steady-state data were simulated on the basis of the steady-state rate equation of the reaction cycle, which was derived on a personal computer (Ericsson PC) by the method of King and Altman [8].

Results

The reaction cycle

The reaction scheme, which has been used in the simulations of the kinetic results, is shown in Fig. 1. It is essentially identical with earlier schemes [4–6], except that ATP binding has been allowed not only in the E_1 but also in the E_2 state. In addition, some steps have been combined into

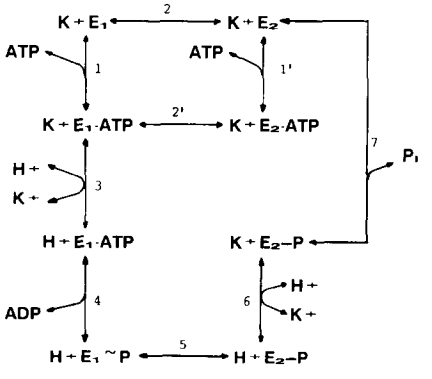

Fig. 1. A reaction cycle of H^+/K^+-ATPase. E_1 and E_2 represent the input and output states of the proton pump, i.e. the state in which H^+ is taken up on side 1 and the enzyme phosphorylated, and the one in which H^+ is given off on side 2 and the enzyme dephosphorylated, respectively.

TABLE I

EQUILIBRIUM AND RATE CONSTANTS IN THE REACTION CYCLE OF Fig. 1 USED FOR THE SIMULATIONS

Step	Equilibrium constant	Forward rate constant	Backward rate constant
1	$2.0\cdot10^6\ M^{-1}$	$1.3\cdot10^7\ M^{-1}\cdot s^{-1}$	
1′	$1.0\cdot10^3\ M^{-1}$	$5.0\cdot10^4\ M^{-1}\cdot s^{-1}$	
2	$5.0\cdot10^{-2}$	$1.7\ s^{-1}$	$35\ s^{-1}$
2′	100	$500\ s^{-1}$	$5\ s^{-1}$
3	$2.5\cdot10^5$	$4000\ s^{-1}$	$500\ s^{-1}$
4	$2.0\cdot10^{-5}$ M	$50\ s^{-1}$	
5	$2.0\cdot10^{-1}$	$42\ s^{-1}$	$200\ s^{-1}$
6	59	$5.0\cdot10^7\ s^{-1}$	$3.4\cdot10^7\ s^{-1}$
7	1.7	$54\ s^{-1}$	

one. The order of the reaction steps takes into account the facts that the kinase reaction is activated by the proton and the phosphatase reaction by the potassium ion. In a sequential mechanism such as this, the actual order does not, however, influence the simulations. Thus, proton binding may, for example, precede ATP binding in E_1. Mg^{2+} is not explicitly included in the scheme, as all experiments have been made at a constant concentration of this ion (2 mM).

The equilibrium and rate constants used in the simulations are listed in Table I, and these may require some comments. The values for the ATP-binding reaction (steps 1 and 1′) are similar to those used by other investigators [9,10] for the simulation of data for the Na^+/K^+-ATPase. Both the affinity and rate have been assumed to be larger in E_1 than in E_2. This has the consequence that K_2 must be smaller than K_2', as thermodynamics requires that $K_1K_2 = K_1'K_2'$. The value of K_3 for the combined reactions of K^+ dissociation and H^+ binding has been arrived at by assuming a pK_a for the H^+-binding group of 6.4 and a dissociation constant for K^+ of 0.1 M, and it is the product of these two equilibrium constants ($10^{6.4} \times 0.1$). In this and other combined reactions, there may seem to be a discrepancy between the equilibrium constant and the rate constants in Table I. This is because the rate constants used in both directions represent the slowest steps in the two combined reactions. In step 4, the phosphorylation reaction and ADP dissociation have been combined into one step, and the rate constant has

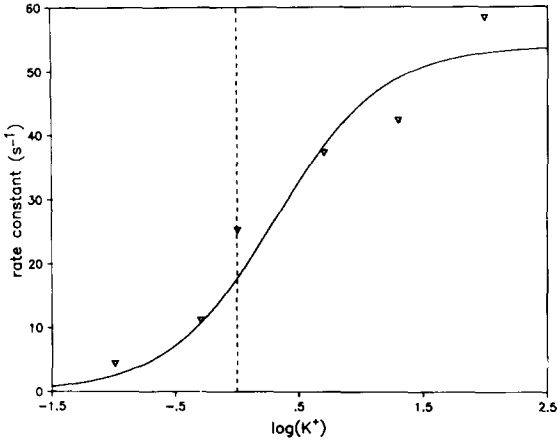

Fig. 2. Dependence of the rate of dephosphorylation of H^+/K^+-ATPase on the KCl concentration. In this and the following figures, the curves are simulated whereas the points are experimental. The experimental data are taken from Fig. 3 in Ref. 4.

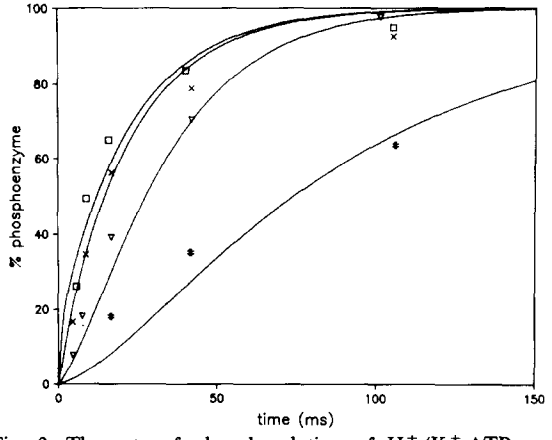

Fig. 3. The rate of phosphorylation of H^+/K^+-ATPase at different ATP concentrations. The experimental data are taken from Fig. 4 in Ref. 4. ATP concentration: #, 1 μM; ▽, 5 μM; ×, 25 μM; □, 100 μM.

been chosen to be consistent with maximum rate of phosphorylation observed experimentally [4]. The constants for step 5 have been adjusted to give the best fit to the experimental points, within the constraints of thermodynamics. The value of K_6 corresponds to a higher affinity for K^+ (590 M^{-1}) and a much lower pK_a (1) compared to step 3. The values for step 7 have been chosen to be consistent with the maximum rate of dephosphorylation [4]. As initial velocities have been used in the steady-state (Fig. 4), product (ADP) concentrations have been assumed to be zero. It should also be noted that the product of all equilibrium constants for a complete reaction cycle has a numerical value of 10^7, which corresponds to the free energy of hydrolysis of ATP at pH 7.4 (60 kJ · mol^{-1}), as required by thermodynamics.

Experimental and simulated kinetics

The effect of K^+ concentration on the dephosphorylation rate is shown in Fig. 2. The deviations between the calculated curve and the experimental points are within the experimental errors. The asymptotic rate at high K^+ concentration is identical with k_7.

In Fig. 3, the rate of formation of phosphorylated enzyme at different ATP concentrations is shown. Again, the agreement between simulated curves and experimental points is quite satisfactory, considering the complexity of the experiment [4].

Eadie-Hofstee plots of steady-state kinetic data from the literature [4] are shown in Fig. 4. It can be seen that the corresponding kinetic equation must be nonhyperbolic, consisting of a sum of two Michaelis-Menten terms with different values of k_{cat} and K_m. To simulate these results we have derived the steady-state kinetic equation for the scheme in Fig. 1 by the King-Altman method [8]. In this equation the kinetic parameters (k_{cat}, K_m) are expressed in terms of the 14 rate constants

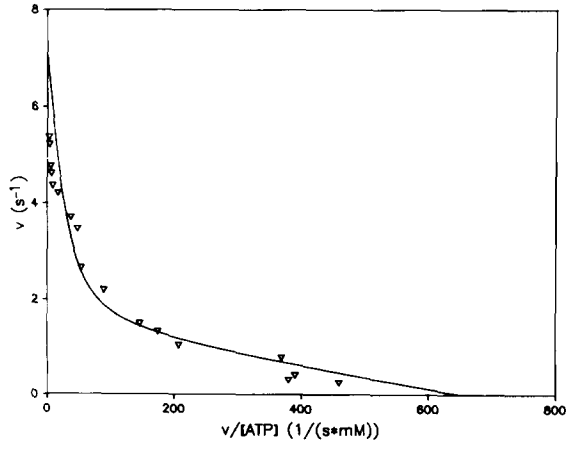

Fig. 4. Eadie-Hofstee plot of the steady-state rates of hydrolysis of ATP catalyzed by H^+/K^+-ATPase. The experimental points have been calculated from the data in Fig. 9 in Ref. 4.

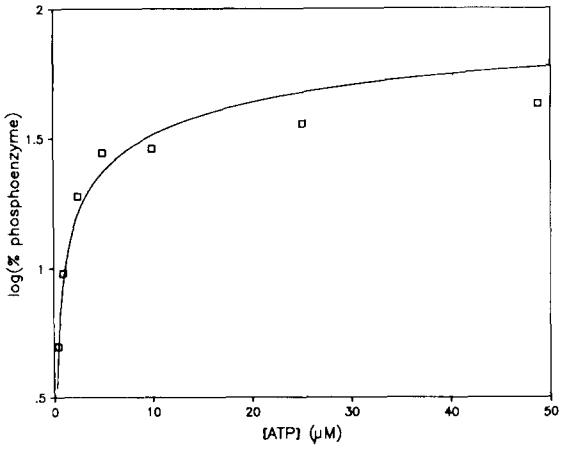

Fig. 5. The dependence of the steady-state concentration of phosphoenzyme on ATP concentration. The enzyme was incubated at 22 °C in 5 mM Pipes-Tris buffer (pH 7.4) containing 2 mM $MgCl_2$, 1 mM KCl and varying concentrations of [γ-^{32}P]ATP. Phosphoenzyme levels were determined at 5 and 20 s according to the procedure described in Ref. 4. The values given are the means of the two determinations. The phosphoenzyme level obtained in the absence of KCl is defined as 100%.

(Table I). The kinetic parameters determined from the simulation are $k_{cat1} = 1.4\ s^{-1}$, $K_{m1} = 2.3\ \mu M$, $k_{cat2} = 5.85\ s^{-1}$ and $K_{m2} = 180\ \mu M$.

The estimated concentration of phosphoenzyme in the steady state at different concentrations of ATP is shown in Fig. 5.

Discussion

The experimental results in Figs. 2–5 are derived from four quite distinct kinds of experiments, two pre-steady-state ones and two in the steady state. The fact that our reaction cycle can be used to simulate all the data satisfactorily with the use of a single set of equilibrium and rate constants provides strong support for the correctness of the essential features in our scheme.

The K^+-dependent dephosphorylation is biphasic [4], but we have only included the rapid phase. The reason for this is that the second phase is too slow to account for the maximum turnover rate at high ATP concentration, and it is thus unlikely to be part of the normal catalytic cycle, e.g. step 5 or 6, as earlier suggested [4]. One possibility is that it is related to the fact that the equilibrium constant for step 7 is not very large, as evidenced by the phosphorylation of the enzyme in the E_2 state by inorganic phosphate [1]. This has the consequence that the rate of step 7 becomes zero before the enzyme has been completely dephosphorylated. The slow hydrolysis still observed could then represent a leak to the less stable $E_1 \sim P$ state.

The simulated curve in Fig. 2 is based on the binding of K^+ to a single site. There is evidence, however, that the functional unit is at least a dimer of the catalytic subunit [11]. The data in Fig. 2 then indicate that the subunits operate independently with identical sites, at least in the phosphatase reaction. The kinetics of the phosphorylation reaction (Fig. 3) can also be accounted for on the basis of a single site.

It has already been pointed out that the biphasic steady-state data in Fig. 4 shows that the kinetic equation must be nonhyperbolic rather than of the simple Michaelis-Menten type. It has been suggested [4] that this is due to the presence of two different active sites, but the pre-steady-state results do not support this, as just discussed. We would like to propose instead that the biphasic kinetics is a direct consequence of the requirement [12] that any pump protein must exist in two conformational states, here designated E_1 and E_2. For the pump to function properly, the affinity for the substrate of the driving reaction (ATP) must be highest in the input state for the ion to be translocated (H^+), i.e. in E_1, but it is unlikely that it becomes zero in the E_2 state. Our simulations (Fig. 4) show that the nonhyperbolic kinetics can be nicely accounted for, if E_2 binds ATP with an affinity which is 2000 times lower compared to E_1. Thus, at low ATP concentration the fastest rate is obtained via the pathway in which the ATP-binding step has a high second-order rate constant (step 1), despite the low rate constant for the conformational change (step 2), whereas at high substrate concentration, where the bimolecular step is rapid even if the rate constant is small (step 1′), it becomes advantageous to follow the pathway involving the rapid conformational transition (step 2′). The same explanation for the biphasic kinetics has been advanced for two other ATP-driven pumps by Reynolds et al. [9].

The parameters k_{cat1} and k_{cat2} represent the catalytic constants for the two pathways just de-

scribed. The actually observed maximum turnover at high ATP concentration is ($k_{cat1} + k_{cat2}$). The value of this sum (7.2 s^{-1}) does not correspond to any of the rate constants used in the simulations (Table I), which illustrates the fact that with very complicated mechanisms it is seldom possible to identify a single rate-limiting step. In the steady-state all steps, of course, occur with the same rate, and the concentration of the intermediates is determined by the rate constants for their decay. If one first-order rate constant is much smaller than all others, then the concentration of the intermediate decaying with this constant will be higher than those of all other intermediates, and this step is said to be rate-limiting. If several rate constants are of the same order of magnitude, however, more than one intermediate state will be significantly occupied, and no single step can be said to limit the rate. In the present case, the rate is thus limited by a number of steps, each with a first-order rate constant of about 50 s^{-1}; this includes some of the bimolecular steps, which at the pH and K^+ concentrations used get apparent first-order constants of this order of magnitude.

Further tests of the validity of the proposed reaction cycle would be obtained, if more of the individual equilibrium and rate constants could be measured directly. Thus, to attempt this would be a fruitful task for future experimentation.

Acknowledgement

This investigation has been supported in part by a grant from the Swedish Natural Science Research Council.

References

1 Sachs, G., Wallmark, B., Saccomani, G., Rabon, E., Stewart, H.B., DiBona, D. and Berglind, T. (1982) Curr. Top. Membr. Transp. 16, 135–160.
2 Norby, J.G. (1987) Chem. Scr. 27B, 119–129.
3 De Meis, L. and Vianna, A.L. (1979) Annu. Rev. Biochem. 48, 275–292.
4 Wallmark, B., Stewart, H.B., Rabon, E., Saccomani, G. and Sachs, G. (1980) J. Biol. Chem. 255, 5313–5319.
5 Stewart, B., Wallmark, B. and Sachs, G. (1981) J. Biol. Chem. 256, 2682–2690.
6 Sachs, G., Kaunitz, J., Mendlein, J. and Wallmark, B. (1988) in Handbook of Physiology, in press.
7 Saccomani, G., Stewart, H.B., Shaw, D., Lewin, M. and Sachs, G. (1977) J. Biol. Chem. 465, 311–330.
8 King, E.L. and Altman, C. (1956) J. Phys. Chem. 60, 1375–1378.
9 Reynolds, J.A., Johnson, E.A. and Tanford, C. (1985) Proc. Natl. Acad. Sci. USA 82, 3658–3661.
10 Tanford, C., Reynolds, J.A. and Johnson, E.A. (1985) Proc. Natl. Acad. Sci. USA 82, 4688–4692.
11 Saccomani, G., Sachs, G., Cuppoletti, J. and Jung, C.Y. (1981) J. Biol. Chem. 256, 7727–2229.
12 Tanford, C. (1983) Annu. Rev. Biochem. 52, 379–409.